sustainability

MDPI

Article

Research on Joint Protection Layers and Gas Prevention Technology in Outburst Coal Seams

Feng Zhang [1,2,*] and Jinshan Zhang [1]

[1] School of Mine and Coal, Inner Mongolia University of Science and Technology, Baotou 014010, China; zjsnkd@126.com
[2] China Coal Technology and Engineering Group Chongqing Research Institute, Chongqing 400037, China
* Correspondence: zfhxq1030@163.com

Abstract: Outburst closed distance coal seam distances are extremely difficult to mine, and are commonly involved in safety accidents in the process of mining. Based on the engineering background of the Wulan Coal Mine at the western margin of the Ordos Basin, this paper presents a theoretical analysis, engineering analogies, and numerical simulations to determine the optimal mining sequence for the Wulan Coal Mine #7, #8, #2, and #3 coal seams. Floor penetration drilling was used to eliminate outbursts in the #7 and #8 coal seams, and gas control in the #2 and #3 coal seams was achieved using ground drilling to pump and release the pressured gas. We established a comprehensive management technology system for gas emissions from the short-distance joint protection layer in the outburst coal seams of Wulan Coal Mine, where pressure relief and drainage were carried out by drilling through the floor and surface drilling pressure relief extraction. Through field tests, the pre-drainage rate of the #2 coal seam in the Wulan Coal Mine was 66.8%, and the pre-drainage rate of the #3 coal seam was 68.1%. This shows that protective layer mining of the #7 and #8 coal seams combined with surface drilling to extract pressure-relief gas can protect the #2 and #3 coal seams.

Keywords: outburst coal mine; closed distance coal seams; mining sequence; outburst prevention measures; gas prevention

Citation: Zhang, F.; Zhang, J. Research on Joint Protection Layers and Gas Prevention Technology in Outburst Coal Seams. *Sustainability* **2022**, *14*, 8859. https://doi.org/10.3390/su14148859

Academic Editor: Giovanna Pappalardo

Received: 5 May 2022
Accepted: 11 July 2022
Published: 20 July 2022

1. Introduction

There are a lot of closed distance coal seams in our country [1–3]. With the increasing depth of coal mining, many mines have been transformed into prominent mines, which are associated with hidden dangers in coal mine production [4–6]. In closed distance coal seams, due to the small distance between the coal seams in addition to the outburst hazard of the coal seam itself, outburst accidents may occur in adjacent coal seams [7–9]. Therefore, there are more outburst hazards and outburst effects in the mining of closed distance coal seams.

Ordos is an important coal production base in China, with coal output from there accounting for about one quarter of the country's production. With the increasing depth and intensity of coal mining in recent years, gas disasters are becoming more and more serious [10–12]. This has been mainly reflected in the following:

(1) The gas pressure and content of coal seams have increased significantly. The gas pressure of the main coal seam generally exceeds 1.5 MPa, the gas content of the coal seam is generally about 8 m^3/t, and with the increase of mining depth, the gas gradient increases rapidly.
(2) The main coal seam is generally gradually upgraded to a coal seam with a higher risk of coal and gas outburst.
(3) During the mining period, the gas gushing volume becomes larger and larger, and the gas gushing of certain working faces now exceeds 100 m^3/min.

(4) The integrity and rationality of regional outburst prevention measures adopted in the early stage need to be improved, and cannot solve the comprehensive outburst prevention problem in the region.
(5) The conventional gas gushing control technical measures put in place in the early stage cannot solve the gas gushing problem of existing mining faces.

Therefore, the effect of gas control has become an important factor affecting the safety, yield, and efficiency of mines in this area. Taking the Wulan Coal Mine as an example, there have been nearly ten coal and gas outburst accidents since the mine was built, causing serious economic losses and casualties. Coal and gas outburst is a complex dynamic phenomenon [13]. The process of coal and gas outburst begins when the outburst coal seam is saturated with gas and is subjected to the comprehensive action of geological tectonic forces, formation pressure, and gas pressure. When mining work occurs close to these areas, the coal gas system that was originally in equilibrium is suddenly destroyed, the elastic potential and free gas are suddenly released, and coal formation cracks greatly increase. The adsorbed gas is desorbed in a large amount in an instant, which further destroys the coal formation, which is pulverized, moves outward, and finally sprays into the roadway with the high-pressure gas flow, forming the outburst of coal and gas [14–16]. Due to the complexity of this prominent mechanism, it is difficult to mine outburst coal seams [17,18]. IF joint outburst prevention is ineffective, and it is very easy for major accidents to occur [19–21].

In this paper, the Wulan Coal Mine is used as a test mine to study comprehensive gas prevention technology for short-distance joint protection layer mining of outburst coal seams. The management of gas disasters, the development and utilization of coalbed methane, and the safe, efficient, and green mining of coal under similar conditions provide the guiding significance of this research.

2. Engineering Background

The Wulan Coal Mine is located in the northern section of the Hulusitai mining area in Alxa Left Banner, Inner Mongolia Autonomous Region. The mine field contains twenty layers of coal seams, including eight mineable coal seams, which are the #2, #3, #5, #6, #7, #8, #10, and #12 coal seams. The total thickness of the coal seams is 23.37 m, and the characteristics of each mineable coal seam are shown in Table 1.

Table 1. Characteristics of each mineable coal seam.

Coal Seam	Average Thickness/m	Distance from the Previous Coal Seam/m	Coal Seam Stability	Roof Stratum	Floor Stratum
#2	3.675	—	Destabilization	Sandy mudstone	Sandstone
#3	9.08	27.83	Stabilization	Siltstone	Sandstone
#5	1.26	22.34	Stabilization	Sandy mudstone	Sandy mudstone
#6	1.22	12.3	Stabilization	Limestone	Sandstone
#7	1.76	37.37	Stabilization	Limestone	Sandy mudstone
#8	2.53	5.95	Destabilization	Mudstone	Sandy mudstone
#10	1.17	25.37	Stabilization	Limestone	Sandy mudstone
#12	1.28	29.46	Destabilization	Sandy mudstone	Sandy mudstone

According to theoretical analysis and field measurement results, the gas occurrence distribution law in Wulan Mine was obtained as follows:

(1) The coal seam occurrence in the east of the syncline is slower than that in the west [22], meaning that the syncline controls the gas occurrence in the east and west areas of the mine. The coal seams to the east of the syncline have a slower occurrence, and the north and south are larger than the central part. For the same coal seam, because the

structure in the north and south of the mine is more complex than in the central part, the overall gas hazard distribution of the mine is higher in the north and south than in the central part.

(2) The differences in the lithology and thickness of the roof and floor of the same coal seam cause gas differences in different regions [23]. For example, the gas content in the sandstone distribution area in the northern part of the #3 coal seam is relatively low.

(3) Different coal seams form different system tracts or different stages of the same system tract, resulting in differences in coal seam thickness, roof, and floor, which in turn affect the coal seam gas content differences [24]. For example, the roof of the #7 coal seam is limestone, and the gas content is relatively low. The #3 and #8 coal seams are respectively formed at the position of the largest flood surface in the Taiyuan Formation and Shanxi Formation transgressive system tract; the thickness of the coal seams is relatively thick, while the permeability of the roof and floor is relatively high, thus the gas content is relatively high and the gas pressure gradient of the #2, #7, #3, and #8 coal seams increases sequentially.

(4) For the same coal seam, with the inclination direction, the gas pressure and gas content increase with the burial depth, and the gas pressure and the burial depth of the coal seam have a roughly positive linear relationship [25].

3. Mining Sequence in Wulan Coal Mine

For Wulan Coal Mine, the vertical distance between the #2 and #3 coal seams of the upper coal seams and the #7 and #8 coal seams of the lower coal seams is large. One protective layer may not protect all the coal seams. It is possible to mine a combined protective layer. Through field investigation and theoretical analysis, the following schemes are proposed for the coal seam mining procedure in Wulan Coal Mine.

The mining sequence of scheme 1 is for the #2, #3, #7 and #8 coal seams, and adopts long borehole pre-drainage along the bedding direction to control the coal seam gas. The #3 coal seam adopts ground drilling to remove the compressed gas, and the #7 and #8 coal seams adopt roof penetration drill holes for gas extraction. The advantages are that the mine resources can be effectively used, the ground is drilled to the roof of the #2 coal seam, the amount of work is minimal, and the output during the adjustment period is larger and more stable. The disadvantage is that the protection effect of the #2 and #3 coal seams for coal seams #7 and #8 is greatly affected by the seam spacing. Due to the large change in the seam spacing and the complex rock structure, there may be areas that cannot be protected.

The mining sequence of scheme 2 is for the #7, #8, #2 and #3 coal seams, of which the #7 and #8 coal seams adopt floor penetration boreholes to eliminate outbursts and the #2 and #3 coal seams adopt surface boreholes for gas drainage. The advantages are that the adjustment period is short, the roadway layout is simple, and the protection effect is less affected by the layer spacing than the scheme 1. The disadvantage is that the output is unstable during the adjustment period.

The mining sequence of scheme 3 is for the #6, #2, #3, #7, and #8 coal seams. The #6, #2, and #3 coal seams adopt surface boreholes for gas drainage, and the #7 and #8 coal seams adopt roof penetration boreholes for gas drainage. The advantage is that the #6 coal seam occurs between the #2 and #3 coal seams and the #7 and #8 coal seams, and mining the #6 coal seam will reduce the outburst risk of the #2, #3, #7, and #8 coal seams, which is beneficial to the future mining layout. The disadvantages are that the initial workload is large and the amount of gas emission from the first working face of the #6 coal seam is large, and exceeds the gas control capacity of the existing technology and equipment.

According to the actual situation of Wulan Coal Mine, scheme 2 is the best scheme, mining with the combined protection layer of the lower group of coal. The mining sequence of the coal seams is thus #7, #8, #2 and #3.

4. Comprehensive Outburst Prevention Technology and Gas Emission Control Technology

4.1. Comprehensive Outburst Prevention Technology

According to the mining sequence of Wulan Coal Mine, the #7 coal seam, which is a protective layer with an outburst hazard, was the first coal seam to be mined, and is close to the underlying #8 coal seam. For the #7 coal seam to achieve safe mining conditions, it is necessary to eliminate outbursts at the #7 and #8 coal seams at the same time. The #7 and #8 coal seams of Wulan Coal Mine are all outburst coal seams, and the measured gas pressure exceeds 2 MPa, which represents a strong outburst hazard.

The #7 and #8 coal seams of Wulan Coal Mine are soft coal seams, and the occurrence is not stable. There are often phenomena such as spray holes, collapse holes, and stuck drills in the construction of bedding drilling. The drilling depth and the hole-forming rate of drilling is low. Using through-bed drilling to pre-drain the coal seam gas is a less technically difficult and more reliable method. Although a floor gas control rock roadway is required for construction, the floor gas control roadway has been arranged, which provides sufficient time and drilling construction for pre-draining coal seam gas. Drilling through the coal seam will not affect the mining operation, which is important for the tension of mining replacement. Moreover, the existence of floor gas control lanes is conducive to the formation of an independent and reliable ventilation system in the mining face of the outburst coal seam. Therefore, the anti-outburst measures give priority to the use of bottom plate penetration drilling and pre-extraction.

According to the above requirements combined with the current roadway layout of the mine, as shown in Figure 1, two floor roadways were arranged in one section, and the floor roadways were arranged in the #12 coal seams at the bottom of the #8 coal seams. One of the floor lanes was arranged near the ventilation roadway and the main pre-drainage of the ventilation roadway and the upper coal seam of the working face. Another floor roadway was arranged near the haulage roadway, mainly pre-draining the haulage roadway and the lower coal seams of the working face.

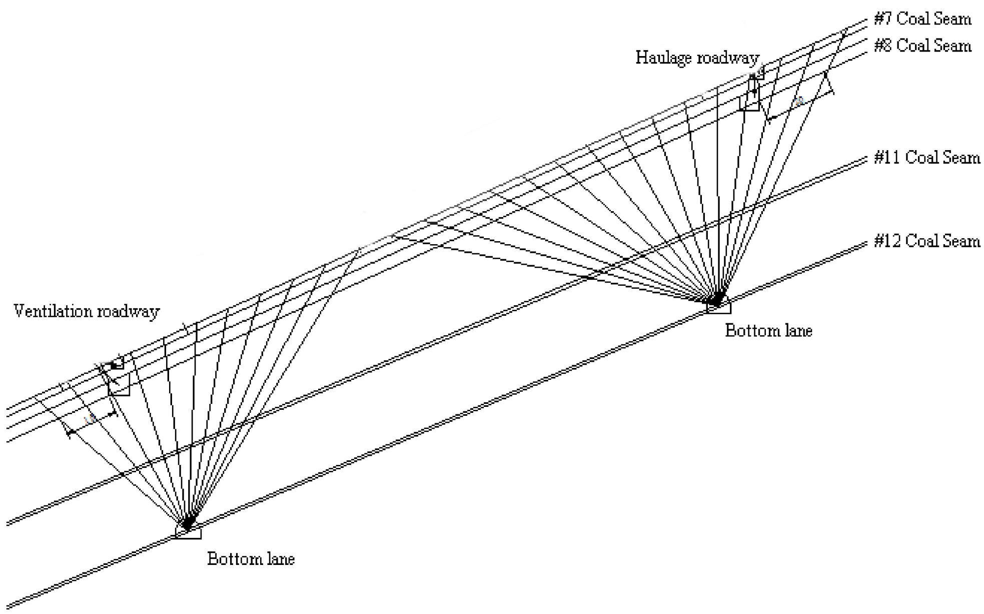

Figure 1. Layout of drilling holes through the floor of #8 coal seam.

4.2. Local Anti-Outbreak Measures

According to the actual situation and the equipment conditions, the anti-outburst measure of the heading face is advanced drilling [26–28]. The layout of the advance drilling is shown in Figure 2 and involves drilling a number of holes in the coal formation in front of the working face while maintaining a certain advance distance between the holes. Then, the coal formation in front of the working face can relieve pressure and drain gas. The borehole is controlled in a range of 25–30 m in front of the working face, and the upper and lower sides of the gently inclined coal seam are each controlled by 5 m. A lead distance of not less than 5 m is reserved during heading. After the advance drilling is completed, the hole is immediately sealed for drainage; the depth of the hole should not be less than 5 m.

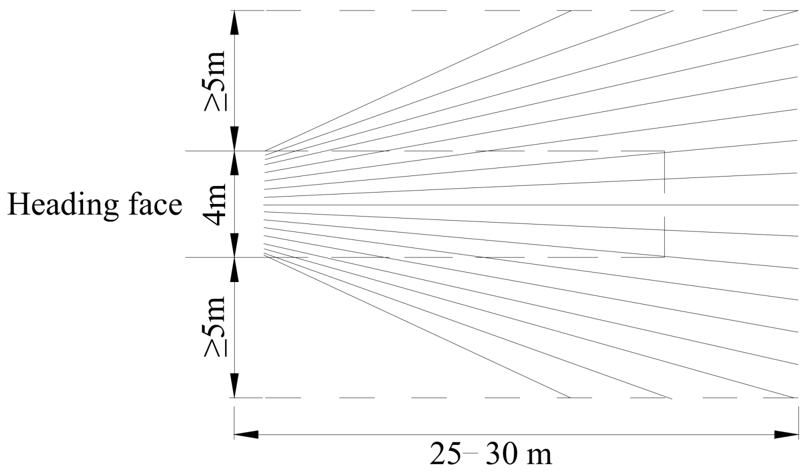

Figure 2. Layout of advanced drilling.

4.3. Gas Control Technology

Comprehensive gas control measures have been adopted for roof strike high drilling and upper corner buried pipes during mining [29–31]. On the basis of the previous monitoring data of Wulan Coal Mine, the above measures can generally solve at least 40 m^3/min of gas gushing from the working face. The general drainage rate of high-position drilling is 15 m^3/min, the drainage rate of the upper corner buried pipe is 10 m^3/min, and the drainage rate while mining is 20 m^3/min. According to the relevant provisions of China's "Coal Mine Safety Regulations", the gas diluted by the return air of the working face should be reduced to below 5 m^3/min. Referring to the experience of relevant domestic engineering practices, it was decided to extend the ground drilling that was originally designed for the #3 coal seam floor to the #7 coal seam roof. In summary, the plan for gas emission control at the II020703 test working face is as follows.

4.3.1. Surface Drilling and Drainage

The principle of pressure relief gas drainage by surface drilling is shown in Figure 3. Drill holes with a diameter of 219 mm were placed on the surface before mining, and the final hole position was 10 m above the roof of the #7 coal seam. Ground boreholes were arranged every 100 m along the direction of the working face in groups of two boreholes. The inner staggered ventilation roadway and haulage roadway was 50 m in length, with a total of 18 surface boreholes. The working face was 5–10 m away from the surface borehole, and the surface pump was used for extraction.

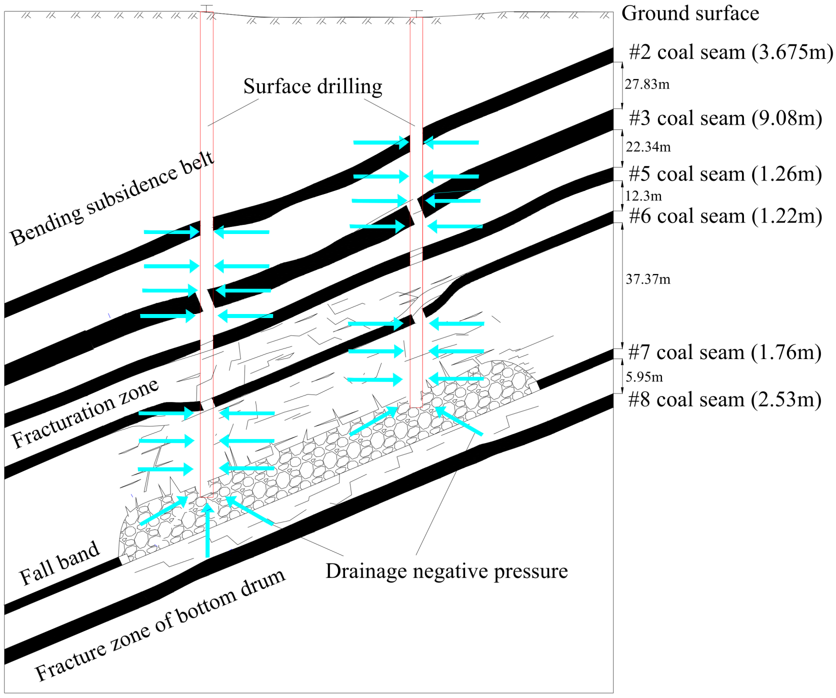

Figure 3. Schematic diagram of pressure relief gas drainage by surface drilling.

4.3.2. Strike High Drilling and Drainage

A drilling field was arranged 40 m along the strike in the II020703 ventilation roadway, and each drilling field was arranged with eight high-level drilling holes. The drilling depth was 60–70 m, the hole diameter was φ94 mm, and the final hole position was above the #7 coal seam at 9–15 m. The overlap length of the front and rear drilling fields was 25 m, and the drilling control range was 30 m above the working face. The layout of the high-position drilling for the II020703 ventilation roadway is shown in Figure 4.

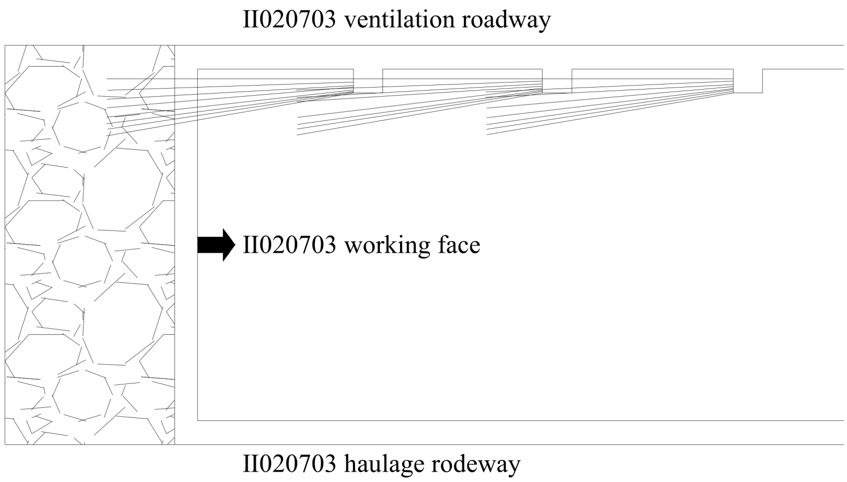

Figure 4. The layout of the high-position drilling.

4.3.3. Gas Drainage by Burying Pipe at the Upper Corner

As shown in Figure 5, a φ450 mm extraction pipeline was arranged in the ventilation roadway before mining and connected with the telescopic air duct set in the upper corner.

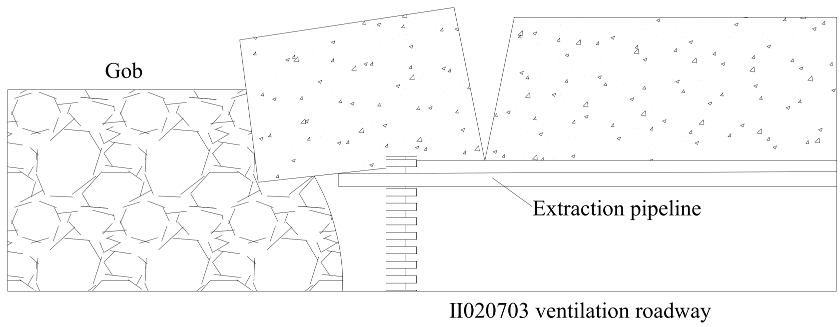

Figure 5. Schematic diagram of upper corner drainage.

4.4. Numerical Simulation

The physical and mechanical parameters of the coal and rock masses are shown in Table 2.

Table 2. Mechanical parameters of coal and rock mass.

Lithologic	Density (kg/m^3)	Bulk (GPa)	Shear (GPa)	Cohesion (MPa)	Tension (MPa)	Friction Angle (°)
Siltstone	2750	21.6	16.8	6.11	2.92	32
Coal	1350	3.17	0.96	1.6	0.71	29
Limestone	2900	30.5	42.4	6.5	3.65	33
Sandy mudstone	2400	9.6	2.69	3	1.8	28
Sandstone	2760	31.5	19.8	5	4	30

A three-dimensional numerical calculation model of Wulan Coal Mine was established based on geological data. The size of the model was 400 × 800 × 349 m. The length of the working face in the #7 coal seam (II020703 face) was 200 m, and coal pillars 100 m wide were left on both sides of the model. The length of the working face in the #8 coal seam (II020803 working face) was 200 m, and the ventilation roadway was arranged 45 m outside the II020703 ventilation roadway. The length along the coal seam strike was 800 m, and 100 m wide coal pillars were left on both sides of the model. The advancing length of the II020703 working face was 600 m. The open cutting of the II020803 working face was misaligned 10 m with the open cutting of the II020703 working face, and the advancing length was 580 m. The height of the model in the Z direction was 350 m. The stress of the overlying strata of the model was 4 MPa. The three-dimensional numerical calculation model is shown in Figure 6.

In the model, four survey lines, A, B, C, and D, were arranged along the inclination of the #2 and #3 coal seams. A set of measuring points was placed every 5 m to record the displacement in the Z direction of the measuring points on the roof and floor of the protected layer. Four survey lines, E, F, G, and H, were arranged along the strike of the #2 and #3 coal seams. A set of measuring points was placed every 10 m to record the displacement in the Z direction of the measuring points on the roof and floor of the protected layer [32,33]. The layout of the measuring points is shown in Figure 7.

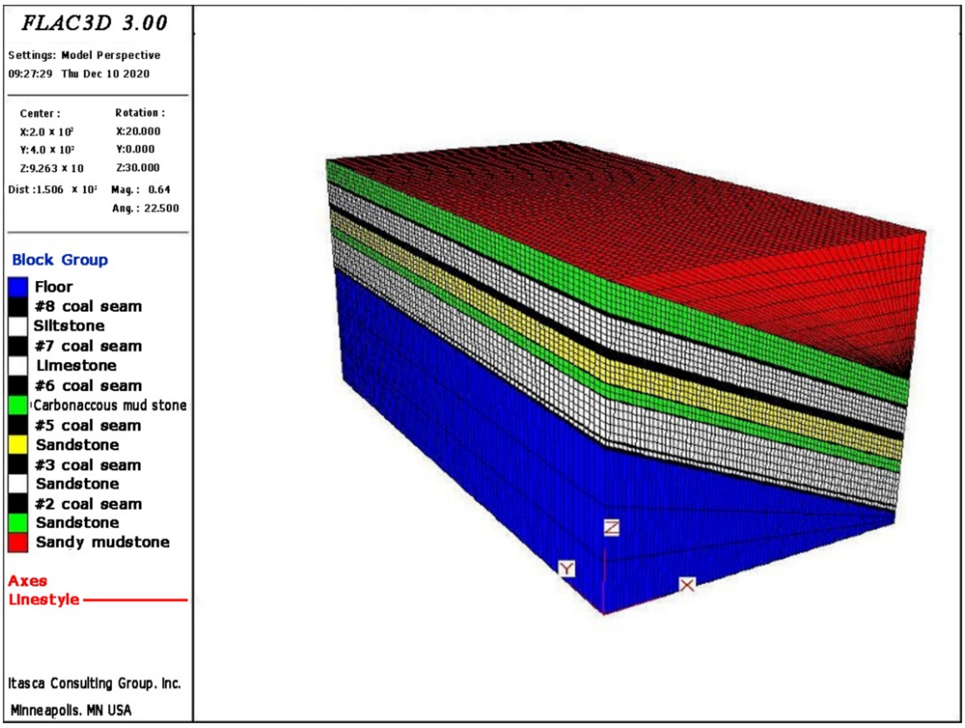

Figure 6. Three-dimensional numerical calculation model.

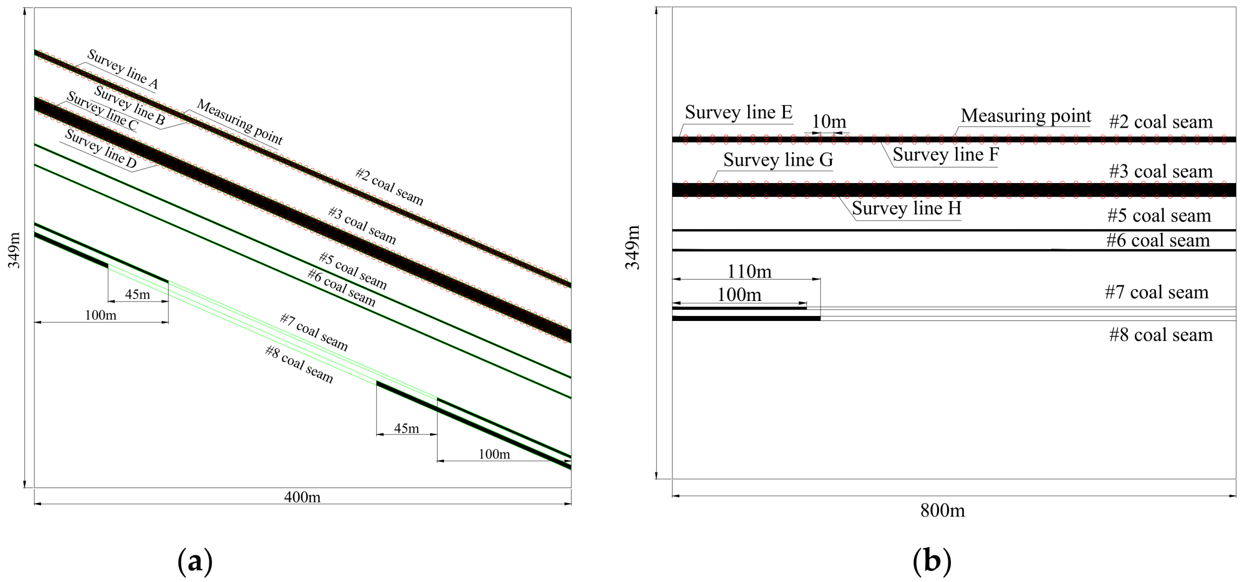

Figure 7. Layout of measuring points: (**a**) model trend measurement point and (**b**) model tendency measurement point.

The numerical simulation results showed that the maximum swelling deformation of the coal seam was greater than the critical point of 3‰. The main calculation results are shown in Figures 8–13.

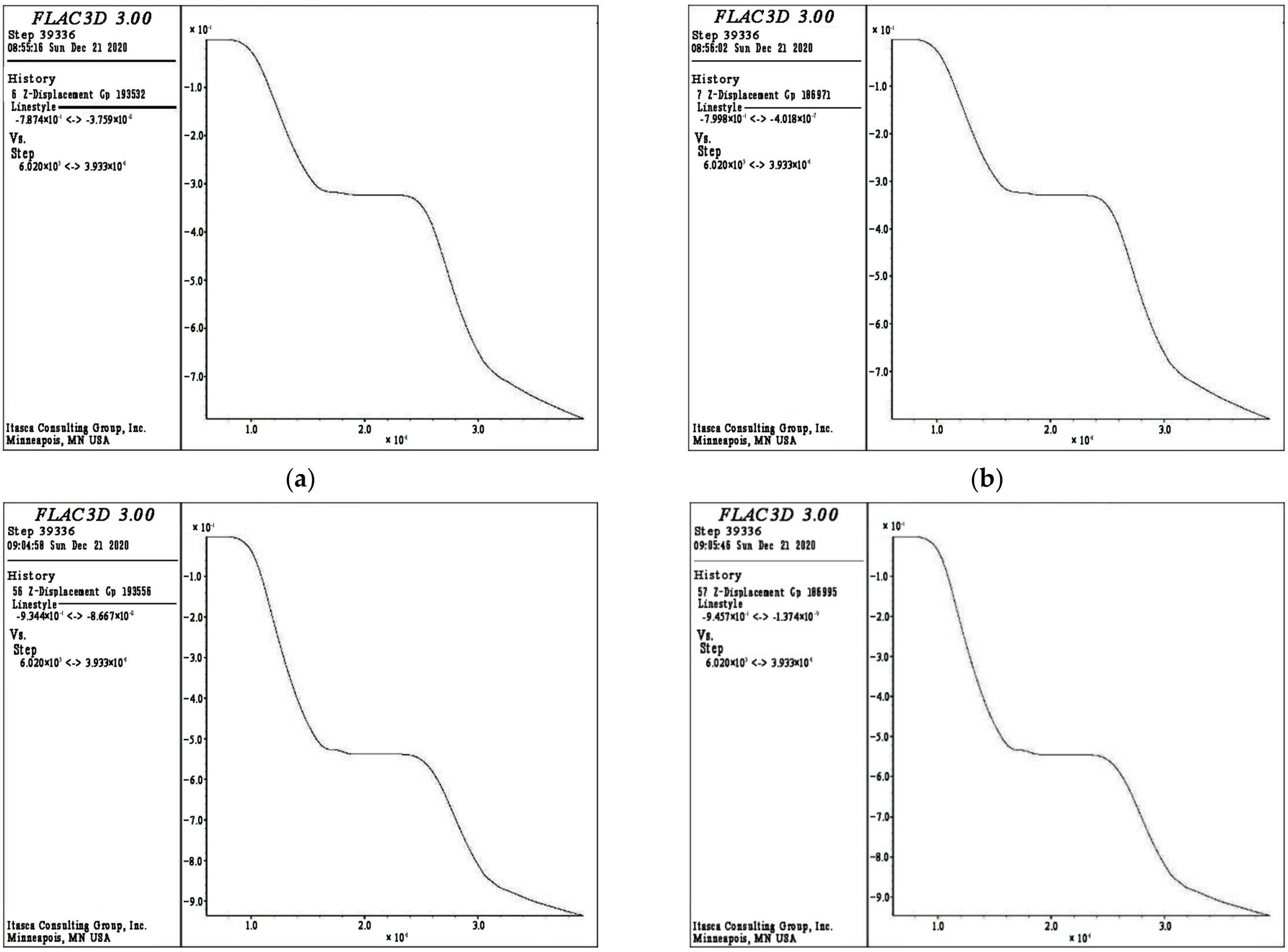

(**a**) (**b**)

(**c**) (**d**)

Figure 8. Displacement of measuring points on roof and floor of #2 coal seam. (**a**) Measuring point (125, 400, 265.7538); (**b**) Measuring point (125, 400, 261.756); (**c**) Measuring point (230, 400, 221.1839); (**d**) Measuring point (230, 400, 217.1861).

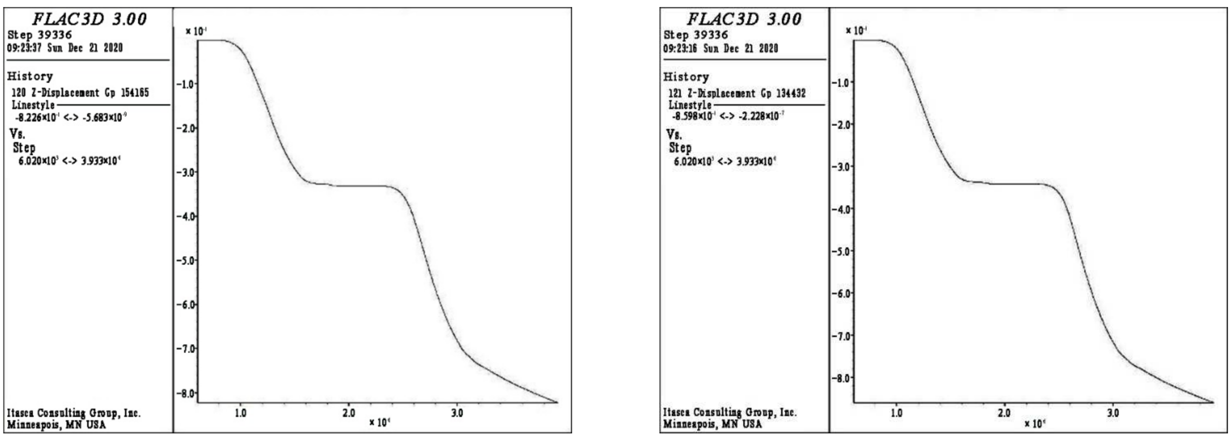

(**a**) (**b**)

Figure 9. *Cont.*

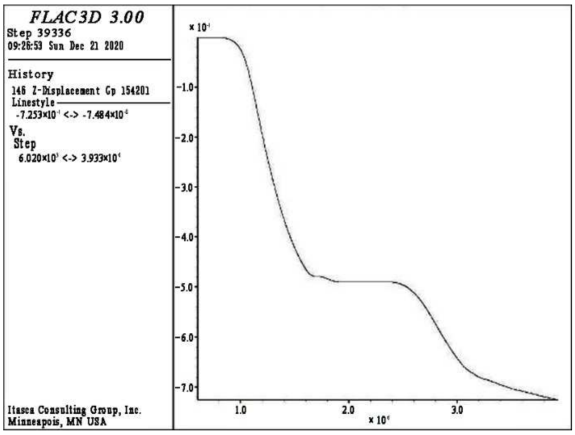

(**c**)

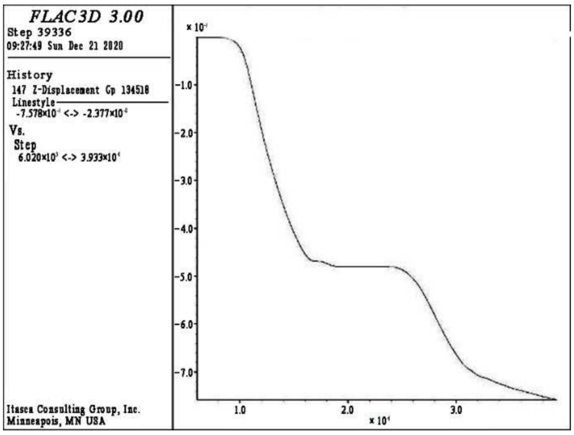

(**d**)

Figure 9. Displacement of measuring points on roof and floor of #3 coal seam. (**a**) Measuring point (100, 400, 242.1344); (**b**) Measuring point (125, 400, 261.756); (**c**) Measuring point (270, 400, 169.9737); (**d**) Measuring point (270, 400, 160.1095).

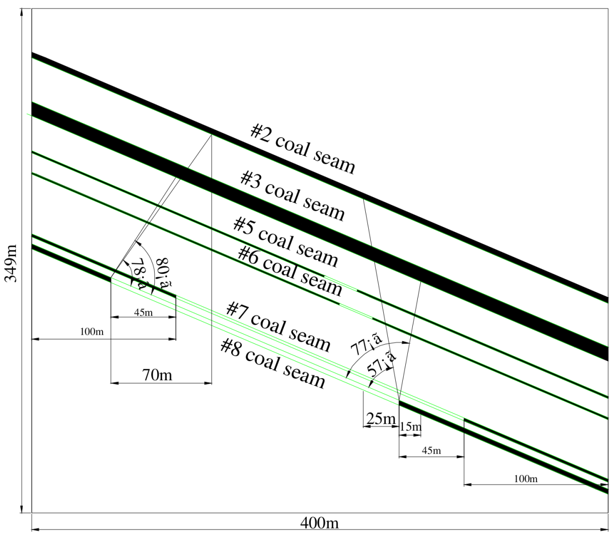

Figure 10. Schematic diagram of protection range in inclined direction.

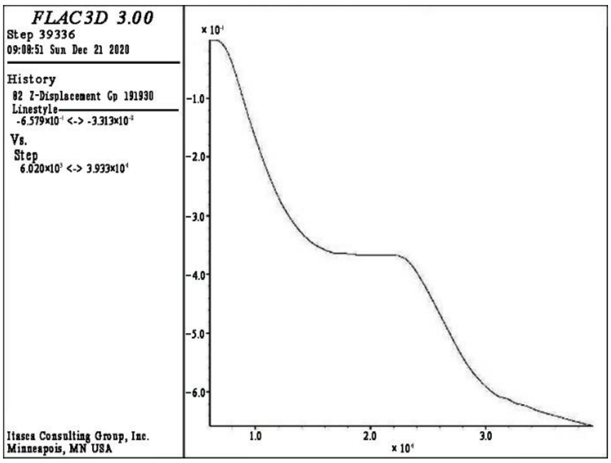

(**a**)

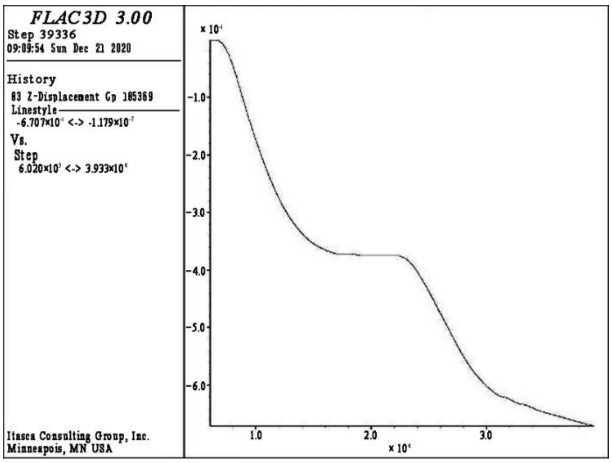

(**b**)

Figure 11. *Cont.*

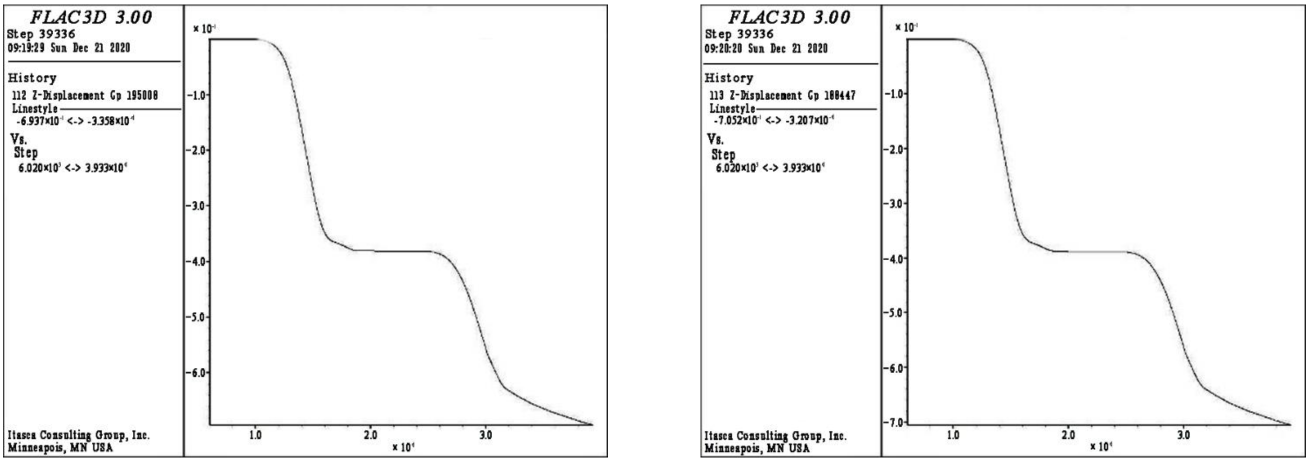

(**c**) (**d**)

Figure 11. Displacement diagram of measured points on the roof and floor of #2 coal seam. (**a**) Measuring point (155, 210, 233.9181); (**b**) Measuring point (155, 210, 229.9203); (**c**) Measuring point (155, 590, 233.9181); (**d**) Measuring point (155, 590, 229.9203).

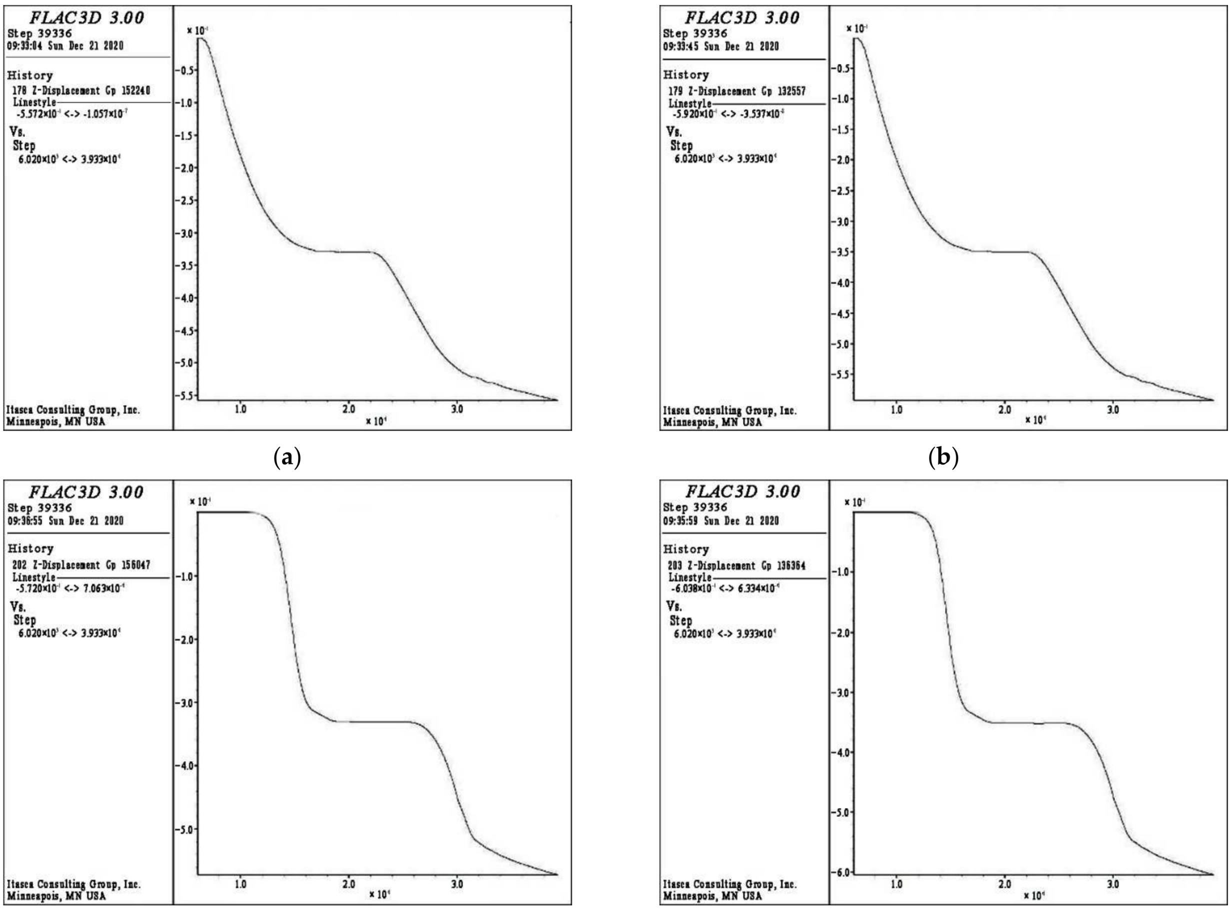

(**a**) (**b**)

(**c**) (**d**)

Figure 12. The #3 coal seam roof and floor measuring point displacement. (**a**) Measuring point (155, 160, 199.6869); (**b**) Measuring point (155, 160, 189.8228); (**c**) Measuring point (140, 620, 199.6869); (**d**) Measuring point (155, 620, 189.8228).

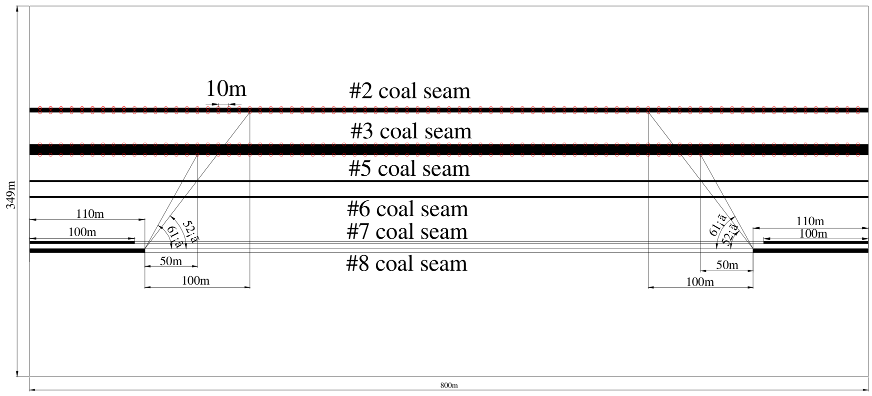

Figure 13. The displacement of roof and floor measuring points in the #3 coal seam.

4.4.1. Protected Area along the Oblique Direction

The upper critical points in the inclined direction of the #2 coal seam were (125, 400, 265.7538) and (125, 400, 261.756). The roof deformation was 0.7874 m, the corresponding floor deformation was 0.7998 m, the thickness of the #2 coal seam was 3.68 m, and the expansion deformation was 3.4‰. The displacement records are shown in Figure 8a,b. The critical points in the lower part of the inclination direction of the #2 coal seam were (230, 400, 221.1839) and (230, 400, 217.1861). The roof deformation was 0.9344 m, the corresponding floor deformation was 0.9457 m, and the expansion deformation was 3.1‰. The displacement records are shown in Figure 8c,d.

The upper critical points in the inclined direction of the #3 coal seam were (100, 400, 242.1344) and (100, 400, 232.2703). The roof deformation was 0.8226 m, the corresponding floor deformation was 0.8598 m, the thickness of the #3 coal seam was 9.08 m, and the expansion deformation was 4.1‰; the displacement records are shown in Figure 9a,b. The lower critical points in the inclination direction of the #3 coal seam were (270, 400, 169.9737) and (270, 400, 160.1095). The roof deformation was 0.7253 m, the corresponding floor deformation was 0.778 m, and the expansion deformation was 3.6‰. The displacement records are shown in Figure 9c,d.

The pressure relief angle of the #3 coal seam calculated according to the numerical simulation and the inclined pressure relief angle of the upper part of the working face, was 80°, and for the lower part of the working face it was 77°. According to the pressure relief angle of the #2 coal seam calculated by numerical simulation, the inclined pressure relief angle of the upper part of the working face was 78° and the inclined pressure relief angle of the lower part of the working face was 57°. As shown in Figure 10, the working face in the #2 coal seam was staggered 70 m in the horizontal direction of the ventilation roadway and 25 m in the haulage roadway to the III020803 working face. The working face in the #3 coal seam was staggered 45 m inside the ventilation roadway and 15 m outside the first haulage roadway to the III020803 working face.

4.4.2. Protected Range along the Strike Direction

The critical points in the strike direction of the #2 coal seam were (155, 210, 233.9181) and (155, 210, 229.9203). The roof deformation was 0.6579 m, the corresponding floor deformation was 0.6707 m. The expansion deformation was 3.5‰, and the displacement records are shown in Figure 11a,b. The critical points where the strike direction of the #2 coal seam is close to the stop line were (155, 590, 233.9181) and (155, 590, 229.9203). The roof deformation was 0.6937 m and the corresponding floor deformation was 0.7052. The expansion deformation was 3.1‰. The displacement records are shown in Figure 11c,d.

The critical points in the strike direction of the #2 coal seam near the open cutting were (155, 160, 199.6869) and (155, 160, 189.8228). The roof deformation was 0.5572 m, the corresponding floor deformation was 0.592 m, and the expansion deformation was 3.8‰; the displacement records are shown in Figure 12a,b. The critical points where the strike direction of the #3 coal seam is close to the stop line were (155, 620, 199.6869) and (155, 620, 189.8228). The roof deformation was 0.572 m, the corresponding floor deformation was 0.6038, and the expansion deformation was 3.5‰. The displacement records are shown in Figure 12c,d.

According to the pressure relief angle of the #2 coal seam calculated by numerical simulation, the strike pressure relief angle at the position of the open cutting and stop line of the III020803 working face was 52°. According to the pressure relief angle of the #3 coal seam calculated by numerical simulation, the strike pressure relief angle at the position of the open cutting and stop line of the III020803 working face was 61°. As shown in Figure 13, the #2 coal seam was within 100 m of the starting mining line and the mining stop line to the III020803 working face. The #3 coal seam was within 50 m of the starting mining line and the mining stop line to the III020803 working face.

5. Field Test

In order to verify the effect of gas prevention, the gas of the #2 and #3 coal seams was drained through surface boreholes to calculate the residual gas amount. The residual gas content of the coal seams was determined by the direct method of the DGC gas content direct measuring device according to the relevant regulations, "Method for Direct Determination of Gas Content in Coal Seams". As shown in Figure 14, the gas content measurement boreholes were arranged at the boundary of the protection area.

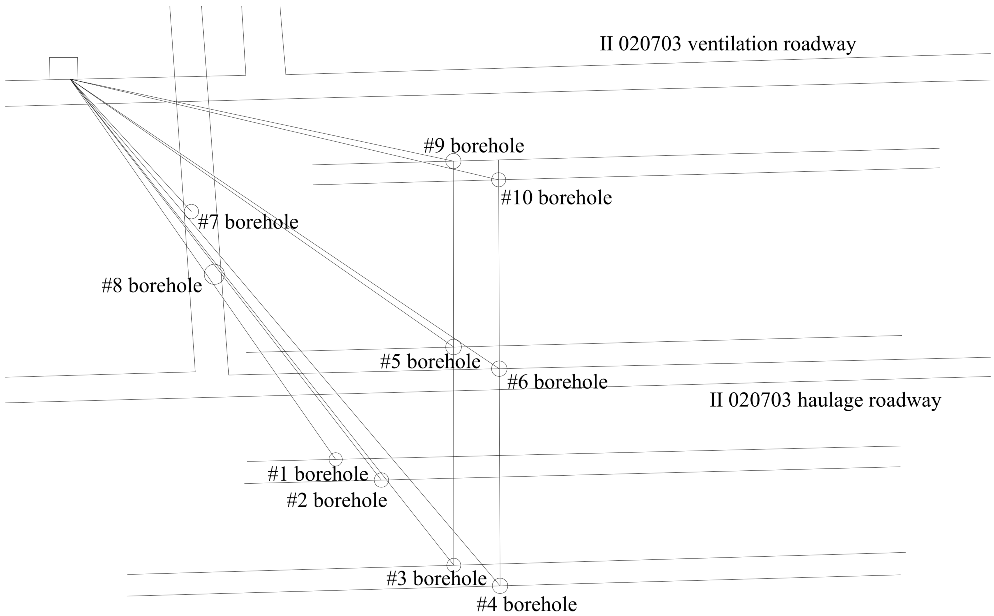

Figure 14. Drilling Layout for Gas Content Determination.

Through the extraction and discharge of gas from the protected layer, the measured residual gas content of the #2 coal seam was 3.24–3.84 m^3/t and the measured residual gas content of the #3 coal seam was 2.72~3.5 m^3/t. The protection of the #2 and #3 coal seams in the protection area was effective. Monitoring data showed that the pre-drainage rate of the #2 coal seam was 66.8% and the pre-drainage rate of the #3 coal seam was 68.1%. This shows that the protective layer mining on the #7 and #8 coal seams combined with surface drilling has a significant effect on gas extraction and can protect the #2 and #3 coal seams.

6. Conclusions

This paper formed a complete set of technology systems suitable for mining gas comprehensive treatment in the outburst coal seam group in Wulan Coal Mine. The main conclusions are as follows:

1. We determined that the mining sequence of Wulan Coal Mine was the #7, #8, #2, and #3 coal seams.
2. We established a comprehensive outburst prevention technology system for closed distance joint protection seams, and we carried out regional pre-drainage and joint outburst prevention for the #7 and #8 coal seams within a limited time for the replacement of mining in Wulan Coal Mine.
3. A gas emission comprehensive treatment technology system involving floor penetration drilling pressure relief interception extraction, surface drilling pressure relief extraction, and high-level drilling extraction was formulated.
4. We analyzed the protection effect of Wulan Coal Mine's close distance combined protection seam mining on the overlying long-distance outburst #2 and #3 coal seams and determined the specific parameters.
5. Field monitoring results showed that the pre-drainage rate of the #2 coal seam in the test area was 66.8% and the pre-drainage rate of the #3 coal seam was 68.1%. This shows that the protective layer mining of the #7 and #8 coal seams combined with surface drilling has a significant effect on gas extraction, and can protect the #2 and #3 coal seams.

Author Contributions: Conceptualization, F.Z.; methodology, J.Z.; software, F.Z.; validation, F.Z.; formal analysis, F.Z.; investigation, J.Z.; resources, F.Z.; data curation, J.Z.; writing—original draft preparation, F.Z.; writing—review and editing, F.Z.; visualization, J.Z.; supervision, J.Z.; project administration, F.Z.; funding acquisition, F.Z. All authors have read and agreed to the published version of the manuscript.

Funding: This research was financially supported by the Higher Educational Scientific Research Projects of Inner Mongolia Autonomous Region (No. NJZY21291).

Institutional Review Board Statement: "Not applicable" for studies not involving humans or animals.

Informed Consent Statement: "Not applicable" for studies not involving humans.

Data Availability Statement: All data included in this study are available upon request by contacting the corresponding author.

Acknowledgments: We are grateful to the anonymous reviewers for their constructive reviews on the manuscript and the editors for carefully revising the manuscript.

Conflicts of Interest: The authors declare no conflict of interest.

References

1. Shang, H.F.; Ning, J.G.; Hu, S.C.; Qiu, P. Field and numerical investigations of gateroad system failure under an irregular residual coal pillar in close-distance coal seams. *Energy Sci. Eng.* **2019**, *7*, 2720–2740. [CrossRef]
2. Ru, W.; Hu, S.; Ning, J.; Wang, J.; Gu, Q.; Guo, Y.; Zuo, J. Study on the Rheological Failure Mechanism of Weakly Cemented Soft Rock Roadway during the Mining of Close-Distance Coal Seams: A Case Study. *Adv. Civ. Eng.* **2020**, *2020*, 8885849. [CrossRef]
3. Yang, X.; Hu, C.; He, M.; Wang, H.; Zhou, Y.; Liu, X.; Zhen, E.; Ma, X. Study on Presplitting Blasting the Roof Strata of Adjacent Roadway to Control Roadway Deformation. *Shock Vib.* **2019**, *2019*, 3174898. [CrossRef]
4. Zhang, A.L.; Zhang, R.; Gao, M.Z.; Zhang, Z.; Jia, Z.; Zhang, Z.; Zha, E. Failure Behavior and Damage Characteristics of Coal at Different Depths under Triaxial Unloading Based on Acoustic Emission. *Energies* **2020**, *13*, 4451. [CrossRef]
5. Hu, C.; Yang, X.; Huang, R.; Ma, X. Presplitting Blasting the Roof Strata to Control Large Deformation in the Deep Mine Roadway. *Adv. Civ. Eng.* **2020**, *2020*, 8886991. [CrossRef]
6. Kholod, N.; Evans, M.; Pilcher, R.C.; Roshchanka, V.; Ruiz, F.; Coté, M.; Collings, R. Global methane emissions from coal mining to continue growing even with declining coal production. *J. Clean. Prod.* **2020**, *256*, 120489. [CrossRef]
7. Zhang, W.; Zhang, D.; Qi, D.; Hu, W.; He, Z.; Zhang, W. Floor failure depth of upper coal seam during close coal seams mining and its novel detection method. *Energy Explor. Exploit.* **2018**, *35*, 1265–1278. [CrossRef]
8. Cui, F.; Jia, C.; Lai, X.; Yang, Y.; Dong, S. Study on the Law of Fracture Evolution under Repeated Mining of Close-Distance Coal Seams. *Energies* **2020**, *13*, 6064. [CrossRef]
9. Zhou, X.; Yang, Y.; Zheng, K.; Miao, G.; Wang, M.; Li, P. Study on the Spontaneous Combustion Characteristics and Prevention Technology of Coal Seam in Overlying Close Goaf. *Combust. Sci. Technol.* **2020**, *194*, 2233–2254. [CrossRef]
10. Jinxian, H.; Zhang, X.; Ma, L.; Hongchen, W.; Aqeel, A.M. Geological Characteristics of Unconventional Gas in Coal Measure of Upper Paleozoic Coal Measures in Ordos Basin, China. *Earth Sci. Res. J.* **2016**, *20*, 1–5.

11. Wang, L.; Lv, D.; Hower, J.C.; Zhang, Z.; Raji, M.; Tang, J.; Liu, Y.; Gao, J. Geochemical characteristics and paleoclimate implication of Middle Jurassic coal in the Ordos Basin, China. *Ore Geol. Rev.* **2022**, *144*, 104848. [CrossRef]
12. Zhifei, L.; Yingchun, W.; Fanghui, H.; Luoping, M.; Xu, J.; Rongfang, Q.; Daiyong, C. Control of accommodation changes over coal composition: Case study of Jurassic medium-thick coal seams in the Ordos Basin, China. *Arab. J. Geosci.* **2020**, *13*, 1–15. [CrossRef]
13. Li, L.; Tang, J.; Sun, S.; Ding, J. Experimental study of the influence of water content on energy conversion of coal and gas outburst. *Nat. Hazards* **2019**, *97*, 1083–1097. [CrossRef]
14. Lu, Z.; Wang, L.; Lv, M.; Lei, Y.; Wang, H.; Liu, Q. Experimental Study on Coal and Gas Outburst Risk in Strong Outburst Coal Under Different Moisture Content. *Front. Earth Sci.* **2022**, *10*, 782372. [CrossRef]
15. Shi, X.Z.; Song, D.H.; Qian, Z.W. Classification of coal seam outburst hazards and evaluation of the importance of influencing factors. *Open Geosci.* **2017**, *9*, 295–301. [CrossRef]
16. Guo, B.H.; Li, Y.Z.; Jiao, F. Experimental study on coal and gas outburst and the variation characteristics of gas pressure. *Geomech. Geophys. Geo-Energy Geo-Resour.* **2018**, *4*, 355–368. [CrossRef]
17. Wang, H.F.; Cheng, Y.P.; Yuan, L. Gas outburst disasters and the mining technology of key protective seam in coal seam group in the Huainan coalfield. *Nat. Hazards* **2013**, *67*, 763–782. [CrossRef]
18. Fisne, A.; Esen, O. Coal and gas outburst hazard in Zonguldak Coal Basin of Turkey, and association with geological parameters. *Nat. Hazards* **2014**, *74*, 1363–1390. [CrossRef]
19. Wang, F.K.; Liang, Y.P.; Zou, Q.L. Correlation between coal and gas outburst risk and adsorption properties of coal seams. *Energy Sci. Eng.* **2018**, *7*, 974–985. [CrossRef]
20. Wang, C.J.; Yang, S.Q.; Li, X.W.; Yang, D.; Jiang, C. The correlation between dynamic phenomena of boreholes for outburst prediction and outburst risks during coal roadways driving. *Fuel* **2018**, *231*, 307–316. [CrossRef]
21. Zhou, H.; Zhang, R.; Cheng, Y.; Dai, H.; Ge, C.; Chen, J. Methane and coal exploitation strategy of highly outburst-prone coal seam configurations. *J. Nat. Gas. Sci. Eng.* **2016**, *23*, 63–69. [CrossRef]
22. Zhang, Z.; Qin, Y.; Yang, Z.; Zhao, J.; Yi, T. Segmentation of multi-coal seam pore structure in single well profile and its sedimentary control: A case study of Well Y1 in Panguan syncline, western Guizhou, China. *Arab. J. Geosci.* **2019**, *12*, 1–16. [CrossRef]
23. Malinnikova, O.N.; Ul'yanova, E.V.; Kharchenko, A.V.; Pashichev, B.N. Influence of Coal Microstructure on Gas Content of the Face Area. *J. Min. Sci.* **2020**, *56*, 351–358. [CrossRef]
24. Zhang, J.; Yang, F.; Zhang, R.; He, J.; Xie, Y.; Miao, Z.; Zhang, J. Experimental Research on Coal Seam Structure and Gas Occurrence Influencing Factors in Weijiadi Mine China. *Fresen. Environ. Bull.* **2022**, *31*, 74–80.
25. Szlązak, N.; Obracaj, D.; Korzec, M. Estimation of Gas Loss in Methodology for Determining Methane Content of Coal Seams. *Energies* **2021**, *14*, 982. [CrossRef]
26. Yang, Z.; Zhang, H.; Li, S.; Fan, C. Prediction of Residual Gas Content during Coal Roadway Tunneling Based on Drilling Cuttings Indices and BA-ELM Algorithm. *Adv. Civ. Eng.* **2020**, *2020*, 1287306. [CrossRef]
27. Ordin, A.A.; Timoshenko, A.M. Coalbed methane release as a function of coal breakup. *J. Min. Sci.* **2016**, *52*, 524–529. [CrossRef]
28. Wang, J.C.; Jiang, F.X.; Meng, X.J.; Wang, X.Y.; Zhu, S.T.; Feng, Y. Mechanism of Rock Burst Occurrence in Specially Thick Coal Seam with Rock Parting. *Rock Mech. Rock Eng.* **2016**, *49*, 1953–1965. [CrossRef]
29. Urashima, K.; Chang, J.S. Removal of volatile organic compounds from air streams and industrial flue gases by non-thermal plasma technology. *IEEE Trans. Dielectr. Electr. Insul.* **2000**, *7*, 602–614. [CrossRef]
30. Kristoffersen, T.T.; Holden, C. Modeling and Control of a Wet-Gas Centrifugal Compressor. *IEEE Trans. Control. Syst. Technol.* **2021**, *29*, 1175–1190. [CrossRef]
31. Rzaev, T.G.; Talybov, E.G.; Teimurov, R.A. Identification of gas dehydration processes and optimal load distribution between technological lines in a dehydrating plant. *Automat. Rem. Contr.* **2005**, *66*, 1861–1867. [CrossRef]
32. Yang, X.; Hu, C.; Liang, J.; Zhou, Y.; Ni, G.; Huang, R. A Case Study on the Control of Large Deformations in a Roadway Located in the Du'erping Coal Mine in China. *Adv. Mater. Sci. Eng.* **2019**, *2019*, 9628142. [CrossRef]
33. Hu, C.W.; Liu, W.; Wang, Y.T. Study on the Influence of the Location of Dirt Band on Top Coal Caving Property in Extra-Thick Coal Seam. *Geotech. Geol. Eng.* **2020**, *38*, 6221–6230. [CrossRef]